MSMOR: Second-Order Alnordi Method for Model Order Reduction with Multiple Non-impulse Sources

Yiyu Shi, Hao Yu and Lei He
Electrical Engineering Department
University of California, Los Angeles 90095
{yshi, hy255, lhe}@ee.ucla.edu

ABSTRACT

1. INTRODUCTION

With current IC technology advances from 90nm to 65 nm, signal and power integrity issue becomes more and more important. The main causes of signal degradation include the voltage and ground bounce. It results when a current surge occurs in a chip, such as when a number of chip outputs switch simultaneously. When the chip's drivers switch, large transient currents go through the chip's package as well as its power grid. Inductance and resistance of the package and power grid create power-supply noise, causing a fluctuation in supply voltage and a voltage variation in the ground plane from true operating voltage, thus influencing the signal and power integrity. To obtain an accurate simulation result and to design a circuit that can function correctly, we need package and power grid co-design and co-simulation.

However, the number of on-chip devices is increasing at an astonishing speed. As a result, the size of the full-chip electrical power grid model has grown exponentially large. The number of metal power grid layers, each with thousands of metal lines and tens of millions of metal sections, is also expanding. The increase of chip size and power grid layer number has caused the design of power delivery system to be more and more complicated. Extracting and simulating package and power grid directly is memory-exhausting and thus impractical. Based upon the well-behaved sparsity, several special-purpose simulators for power grids or package are proposed, like in [1]. However, when the low content frequency is in dominance, those techniques are not efficient since they need to choose a sufficiently small timestep.

Model order reduction technique is another way to reduce the memory requirement and to speed up the simulation. Typical model order reduction methods include PRIMA [2], Block SAPOR [3], etc. But if we apply those methods directly to P/G grid and package cases, they will not work well. One main reason for this is they match the moments of original circuit block by block. If the circuit has n I/O ports, then they match the first $\lfloor \frac{q}{n} \rfloor$ if the circuit is reduced to order q. When n is very large, which is actually the case in power grid and package, those methods cannot match high order block moments, leading to a loss of accuracy. In addition, the runtime of those methods heavily depends on the number of sources.

We note that during the course of simulation, we are only interested in the output vector when the circuit is excited by certain input vector. We do not need to match the first q block moments of transfer function exactly. Instead, we can only match the moments of the output vector. Led by this idea, several methods are being proposed to deal with circuit with multiple sources, like EKS [4] and IEKS [5]. They employ incremental orthogonalization algorithm and implicitly match the moments of output vector. Those methods solve the problem brought by multiple sources. However, accumulative errors might occur during the incremental orthogonalization process, which is in detail analyzed in the next section.

In addition, IEKS can only deal with current sources without $\frac{1}{s^i}$ terms such as PWL, which limits its application as some common sources, like sine and attenuated sine wave forms, do have such terms. EKS, on the other hand, have to expand the Laplace transformation of those sources into series and select the dominant terms. This surely leads to inaccuracy.

Another problem that exists with EKS and IEKS is that they cannot deal with RCS circuits. With the increase of the operating frequency of the state-of-the-art IC chips, it becomes more and more important to study the magnetic coupling effect. The traditional methods are based on partial inductance concept, and the resulting matrix is usually large and dense [6], which may cause computational difficulties. If we use susceptance matrix instead, it is usually diagonally dominant and can be sparsified by a simple truncation method without disrupting the positive definiteness [7]. Both EKS and IEKS are in essence first-order model order reduction method. Therefore, if we apply EKS or IEKS directly to reduce an RCS circuit, it will not guarantee passivity. Hence, a second-order model order reduction method with multiple current sources is in high demand.

To solve the problems of multiple sources and model order reduction on RCS circuit at the same time, we develop an accurate yet efficient second-order Arnoldi method for passive model order reduction on RCS circuits with multiple sources, namely SAPOR. It can deal with all kinds of RHS sources without performing moment shifting and incremental orthogonalization algorithm; It can handle RCS circuit with multiple current sources. Experiments show that it is numerically more stable, more accurate and more efficient.

The rest of this paper is organized as follows. In Section 2, we review and analyze the two MOR methods with multiple sources. Our new method, MSMOR, is presented and analyzed in Section 3. Several numerical examples and a package and power grid co-simulation example are provided in Section 4. Concluding remarks are given in Section 5.

2. PRELIMINARY

Consider a modified nodal formulation (MNA) of a linear circuit. In the Laplace domain, it can be expressed as:

$$\begin{aligned} \mathcal{G}x(s) + s\mathcal{C} &= \mathcal{B}u_e(s) \\ y_e(s) &= \mathcal{B}^T x(s) \end{aligned} \quad (1)$$

, where $\mathcal{G} = \begin{bmatrix} G & E_s^T \\ -E_s & \mathbf{0} \end{bmatrix}$, $\mathcal{C} = \begin{bmatrix} C & \mathbf{0} \\ \mathbf{0} & L \end{bmatrix}$, and $\mathcal{B} = [B, \mathbf{0}]$.

Many model order reduction methods, like PRIMA [2], SAPOR [3] all perform reduction on the transfer function, i.e.

$$H(s) = \mathcal{B}^T(\mathcal{G} + s\mathcal{C})^{-1}\mathcal{B} \quad (2)$$

However, performing direct reduction on H(s) without considering RHS sources will cause the runtime to be heavily depend on the number of ports. What is more, when the port number is very close to the number of nodes, it can only match the first one or two block moments of the original system, and cannot guarantee high accuracy.

When a block moment of the transfer function $H(s)$ is matched by $\widehat{H}(s)$ to order q, exactly we need to match q^2 moments, q moments for each $\widehat{H}_{i,j}(1 \le i, j \le q)$. Then the reduced tranfer function $\widehat{H}(s)$ is used to calculate the output, $y_e(s) = \widehat{H}(s)u_e(s)$. In most cases, we are only interested in matching the output of the circuit. That is to say, we only need to match the first q moments of the output, instead of match the $q \times q^2$ moments (q block moments) of the tranfer function.

Only considering output matching, [4] is proposed to find Extended Krylov Subspace (EKS) for reduced order analysis of linear circuits with multiple piecewise linear (PWL) sources. It expresses the PWL source as a sum of delayed ramps in the Laplace domain,

$$u(s) = \frac{1}{s^2}\sum_{i=0}^{k} r_i exp(-\tau_i s) \quad (3)$$

This expression contains $\frac{1}{s}$ and $\frac{1}{s^2}$ terms which become obstacle for the traditional Krylov subspace methods. EKS solves this problem by shifting the moments towards right in the frequency spectrum of u(s). This results in a loss of accuracy, which is shown in [5]. Another problem existing with EKS is that when dealing with current sources of common forms, like

$$\begin{aligned} u_1(t) = sin(\omega t) \qquad & L(u_1) = \frac{\omega}{s^2+\omega^2} \\ u_2(t) = e^{-\alpha t}cos\omega t \qquad & L(u_2) = \frac{s+\alpha}{(s+\alpha)^2+\omega^2} \end{aligned} \quad (4)$$

it needs to expand the Laplace transformation of u(t) and take the first several moments as an approximation before performing moment shifting. This procedure is obviously error-prone. To improve EKS, IEKS is proposed in [5]. It is proved that given a finite-time PWL source, IEKS constructs its moment representations with zero -1_{st} and -2_{nd} order moments. However, IEKS cannot handle RHS sources with non-zero s^i moments like (4).

More importantly, we note that both EKS and IEKS use the incremental orthogonalization algorithm to find the projection basis. This algorithm, however, is numerically unstable and inaccurate. To illustrate it, recall the orthogonalization procedure in [4]. The new vector r_i for the orthogonomal basis is generated as following:

$$r_i = G^{-1}(\prod_{j=0}^{i-1}\alpha_j\mathcal{B}\bar{u}_i - \mathcal{C}(\widehat{r}_1 + \alpha_{i-1}\sum_{j=0}^{i-1}h_{i-1,j}\widehat{r}_j)) \quad (5)$$

For the simplicity of presentation, we denote $\mathcal{R} = G^{-C}$. The incremental orthogonalization algorithm suffers from numerical stability and accuracy problems. To illustrate it, we assume that the directions of the orthogonormalized basis, $\widehat{r}_i$, will not be significantly influenced by the calculation error. But their norms are not strictly equal to 1. This assumption is reasonable because the entries in $\bar{r}_i$ are very close to zero and calculating their norms is error-prone in real cases. If minor error happens when we calculate $\alpha_0 = \frac{1}{||\mathcal{R}\bar{u}_0||}$ and we get $\tilde{\alpha}_0 = \alpha_0 + \delta\alpha_0$, then from (5), we have $\bar{r}_1 = r_1 + \mathcal{R}\bar{u}_0\delta\alpha_1$ According to our assumption, the orthogonalized vector $\bar{r}_1$ will have the same error bound because the orthogonal process is in fact projecting r_1 along the direction represented by $\widehat{r}_0$. The result is not related to the norm of $\widehat{r}_0$. Therefore,

$$\begin{aligned} \tilde{\alpha_1} &= \frac{1}{||\bar{r}||} = \frac{1}{||\bar{r_1} + \mathcal{R}\bar{u}_0\delta\alpha_0||} \\ &\ge \frac{1}{||\bar{r_1}|| + ||\mathcal{R}\bar{u}_0\delta\alpha_0||} \\ &= \frac{1}{||\bar{r_1}||}\frac{1}{1 + \frac{||\mathcal{R}\bar{u}_0\delta\alpha_0||}{||\bar{r_1}||}} \\ &= \frac{1}{||\bar{r_1}||}(1 - \frac{||\mathcal{R}\bar{u}_0\delta\alpha_0||}{||\bar{r_1}||} + \cdots) \end{aligned} \quad (6)$$

Accordingly, we get $\tilde{\alpha_1} = \alpha_1 + \delta\alpha_1$, where $\delta\alpha_1 = \frac{||\mathcal{R}||}{||\alpha_1||^2}u_0\delta\alpha_0$ In general, we can get the similar recursive relationship between $\delta\alpha_i$ and $\delta\alpha_{i-1}, \delta\alpha_{i-2}, \cdots, \delta\alpha_0$ from (5), which shows how the error is propagated and amplified during the course of recursion:

$$\delta\alpha_i = \frac{||\mathcal{R}||}{||\alpha_i||^2}\sum_{k=0}^{i-1}\bar{u}_k\delta\alpha_k \quad (7)$$

Finally, IEKS and EKS cannot deal with RCS circuits, which significantly limit their application, as have discussed in the previous section.

3. MSMOR METHOD

In this section, we present our MSMOR method to perform model order reduction considering all kinds of current sources for an RCS circuit. Since the susceptance matrix can be regarded as the inverse of the inductance matrix, we can write the system equation of an RCS circuit as in [8]

$$\begin{aligned} (sC + G + \frac{1}{s}\Gamma)V(s) &= BJ(s) \\ Y(s) &= B^T V(s) \end{aligned} \quad (8)$$

where $\Gamma = E_s S E_s^T$ If we denote N as the circuit nodes excluding the ground nodes, and p as the port number, then $V(s)$ is the state variable vector, G and C ($\in R^{N\times N}$) are state matrices, B ($\in R^{N\times p}$) is the port incident matrix, and J ($\in R^p$) is the input current vector.

3.1 Current Source Classification and System Transformation

Each entry $\bar{J}(s)$ in vector J indicates the Laplace Transformation of one independent current source. We divide

those current sources into two categories: rational (denoted as R-source) and irrational (denoted as I-source) according to their Laplace Transformations. Typical R-sources that are common in physical design include (attenuated) trigonometric sources like $sin(\omega t)$, $e^{-\alpha t}sin(\omega t)$, etc. Their Laplace transformations can be expressed as rational function of s:

$$\bar{J}(s) = \frac{\bar{a}_0 + \bar{a}_1 s + \cdots + \bar{a}_n s^n}{\bar{b}_0 + \bar{b}_1 s + \cdots + \bar{b}_n s^m} \tag{9}$$

Typical I-sources that are common in physical design include impulses, PWL sources, etc. The Laplace transformations of those sources cannot be expressed in rational form like R-sources.

To deal with the I-sources, we first expand them into series and take the dominant n+1 terms (from s^{-m} to s^{n-m}) as an approximation.

$$\bar{J}(s) = \sum_{i=0}^{n} \bar{J}_i s^{i-m} \tag{10}$$

Experiments show that $n = 3$ can provide a maximum error less than 10^{-4}. $\bar{J}(s)$ now can be viewed as (9) with $b_0, b_1, \cdots, b_{n-1}$ all equal to zero. and from now on we will discuss how to deal with R-sources in the form of (9).

Use (9) and J(s) can be written as:

$$J(s) = \frac{1}{b_0 + b_1 s + \cdots + b_n s^m} \begin{pmatrix} \sum_{i=0}^{n_1} a_i^1 s^i \\ \vdots \\ \sum_{i=0}^{n_p} a_i^p s^i \end{pmatrix} \tag{11}$$

Inserting (11) into (8) gives

$$\sum_{i=0}^{m+1} \Upsilon_i s^i V(s) = \sum_{i=0}^{n} \Theta_i s^i \tag{12}$$

where Υ_i and Θ_i can be directly calculated by expanding the polynomial product: $\Upsilon_i = Cb_{i-1} + Gb_i + \Gamma b_{i+1}, \Theta_i = B[a_i^1, a_i^2, \cdots, a_i^p]^T$.

If in (12)the highest order of s in LHS is smaller than that of RHS, then we cannot directly perform system linearization which will be discussed in the next subsection. We first introduce a set of auxiliary variables V_i $(i = 1, 2, \cdots, n-m)$ to raise the order of LHS in (12)

$$\begin{aligned} V(s) &= sV_1 \\ V_1 &= sV_2 \\ &\cdots \\ V_{n-m-1} &= sV_{n-m} \end{aligned} \tag{13}$$

Set $U = [V, V_1, V_2, ...V_{n-m}]^T$ as a new state vector, and we can transform the system equation into the following format:

$$\begin{aligned} TU &= K\sum_{i=0}^{n} \Theta_i s^i, \\ Y &= K^T U \end{aligned} \tag{14}$$

where $T = \begin{bmatrix} I & -sI & & & \sum_{i=0}^{m+1} \Upsilon_i s^{i+n-m} \\ & I & -sI & & \\ & & \ddots & & \\ & & & I & -sI \end{bmatrix}$ $(\in R^{N(n-m+1)\times N(n-m+1)})$; and $K = \begin{bmatrix} B & \mathbf{0} & \dots & \mathbf{0} \end{bmatrix}^T$ $(\in R^{(N(n-m+1)\times p)})$. The new system is equivalent to the original one, except for the increased dimension.

T can further be decomposed according to the descending order of s:

$$T = \Psi_{n+1} s^{n+1} + \Psi_n s^n + \cdots + \Psi_1 s + \Psi_0 \tag{15}$$

where $\Psi_i = \begin{cases} \begin{bmatrix} \mathbf{0} & \Upsilon_i \\ \mathbf{0} & \mathbf{0} \end{bmatrix} & i \geq 2 \\ \begin{bmatrix} \mathbf{0} & \Upsilon_1 \\ \mathbf{0} & \mathbf{0} \end{bmatrix} + \begin{bmatrix} \mathbf{0} & \mathbf{0} \\ \mathbf{0} & -I \end{bmatrix} & i = 1 \\ \begin{bmatrix} \mathbf{0} & \Upsilon_0 \\ \mathbf{0} & \mathbf{0} \end{bmatrix} + \begin{bmatrix} \mathbf{0} & \mathbf{0} \\ I & \mathbf{0} \end{bmatrix} & i = 0 \end{cases}$

Inserting (15) into the new system equation (14), the system equation can be rewritten in the descending order of s term:

$$\begin{aligned} \sum_{i=0}^{n+1} \Psi_i s^i U &= K \sum_{i=0}^{n} \Theta_i s^i \\ Y &= K^T U \end{aligned} \tag{16}$$

Note that if in (12) LHS has a higher order than RHS, then it is not necessary to raise the order of LHS and () can be directly obtained.

3.2 System Linearization

Shifting (3.1) with $s = s_0 + \sigma$, we have

$$\sum_{i=0}^{n+1} A_i \sigma^i U(\sigma) = \sum_{i=0}^{n} K_i \sigma^i \tag{17}$$

where $A_i = \sum_{k=i}^{n+1} C_k^i \Psi_i s_0^{k-i}$ and $R_i = \sum_{k=i}^{n} C_k^i s_0^{k-i} i\Theta_i$. These coefficient matrices can be directly derived from polynomial expansion in (3.1).

Again introduce a set of new variables $Z_i(\sigma)(i = 1, \cdots, n)$ satisfying

$$\begin{aligned} A_{n+1}U(\sigma) + \sigma Z_n &= R_n \\ \sigma(A_n U - Z_n) + Z_{n-1} &= R_{n-1} \\ \sigma(A_{n-1}U - Z_{n-1}) + Z_{n-2} &= R_{n-2} \\ &\cdots \\ \sigma(A_2 U - Z_2) + Z_1 &= R_1 \end{aligned} \tag{18}$$

Substituting (18) into (17), we have

$$(A_0 + A_1\sigma)U - \sigma Z_1 = R_0 \tag{19}$$

Combing (19) and (18) and noticing that the first N rows of U is exactly the original state variable V in (8), we get

$$(I - \sigma A) \begin{bmatrix} V \\ D \end{bmatrix} = \begin{bmatrix} q_0 \\ p_0 \end{bmatrix} \tag{20}$$

where $A = \begin{bmatrix} -A_0^{-1}A_1 & A_0^{-1} \\ -A_{n-1} & \\ -A_{n-2} & \\ \vdots & I \\ -A_2 & \end{bmatrix}$; $D = \begin{bmatrix} U(N+1:(n-m)N) \\ Z_n \\ \vdots \\ Z_1 \end{bmatrix}$

and if we denote $M = \begin{bmatrix} A_0^{-1}R_0 & R_n & R_{n-1} & \cdots & R_1 \end{bmatrix}^T$, then $q_0 = M(1:N)$ and $p_0 = M(N+1:(n+1)(n-m)N$

By moving $(I - \sigma A)$ to the RHS of (20) and performing a Maclaurin series expansion, we have

$$\begin{bmatrix} V \\ D \end{bmatrix} = (I + \sigma A + \sigma^2 A^2 + \cdots) \begin{bmatrix} q_0 \\ p_0 \end{bmatrix} \tag{21}$$

Obviously, $A^{i-1}\begin{bmatrix} q_0 \\ p_0 \end{bmatrix}$ is the i-th moment of $\begin{bmatrix} V \\ D \end{bmatrix}$, q_0 and p_0 are actually the first moments of V and R, respectively.

Equation (20) is a linearized form of (17) with RHS independent of σ. If $\begin{bmatrix} V \\ D \end{bmatrix}$ is the solution of (20), then V must be the solution of (12). Therefore, the upper part of the i-th moment $\begin{bmatrix} V \\ D \end{bmatrix}$, i.e. $\begin{bmatrix} I & \mathbf{0} \end{bmatrix} A^{i-1}\begin{bmatrix} q_0 \\ p_0 \end{bmatrix}$, should be equal to the i-th moment of the output V. A rigid proof is provided in the following subsection.

3.3 Projection

In order to construct an orthonormal basis q_i for the projection matrix Q, we employ a similar procedure as the SOAR algorithm presented in [9]. Once we obtain Q, we perform an orthogonal projection on the original second-order system (8), and get the reduced-order system of the same form.

$$\begin{aligned} (s\widehat{C} + \widehat{G} + \frac{1}{s}\widehat{\Gamma})\widehat{V}(s) &= \widehat{B}J(s) \\ Y(s) &= \widehat{B}^T\widehat{V}(s) \end{aligned} \tag{22}$$

where $\widehat{C} = Q^TCQ$, $\widehat{G} = Q^TGQ$, $\widehat{\Gamma} = Q^T\Gamma Q$, $\widehat{V} = Q^TV$ and $\widehat{B} = Q^TB$. Since C, G, Γ are all symmetry positive semi-definite, it is proven in [10] that the orthogonal projection preserves the passivity of the original system. And we can conclude that the reduced-order system in (22) has guaranteed passivity, too.

3.4 Numerical Analysis of MSMOR

First we formalize the effectiveness of MSMOR by the following two theorems.

*Theorem*1. For single-input-single-output (SISO) system, if the q columns of projection matrix Q are obtained from a generalized SOAR procedure, then the transfer function $\widehat{H}(s)$ after projection can match the first q moments of the original transfer function $H(s)$.

Proof. See [8].

*Theorem*2. For multiple-input-multiple-output (MIMO) system, MSMOR can exactly match the first q moments of the output V if the projection matrix Q has q columns.

Proof. Decompose $J(s) = J_0 + J_1s + J_2s^2 + \cdots$, where $J_i(\in R^{p\times 1})$. We note that the following two systems are equivalent.

$$\begin{aligned} (Gs + C + \frac{\Gamma}{s})V(s) &= BJ(s) \\ Y(s) &= B^TV(s) \end{aligned} \tag{23}$$

$$\begin{aligned} (Gs + C + \frac{\Gamma}{s})V(s) &= B'_0 + B'_1s + B'_2s^2 + \cdots \\ Y(s) &= (B'^T_0 + B'^T_1s + \cdots)V(s) \\ B'_i &= BJ_i \end{aligned} \tag{24}$$

Apply the superposition theorem, (24) can be decomposed into several subsystems, each in the form of

$$\begin{aligned} (Gs + C + \frac{\Gamma}{s})V_i(s) &= B'_is^i \\ Y_i(s) &= B'^T_is^iV(s) \end{aligned} \tag{25}$$

and

$$Y = Y_0 + Y_1 + \cdots \tag{26}$$

MSMOR finds projection matrix Q_i for each subsystem in (25), the input of which is s^i. And $Q = Q_1 + Q_2 + \cdots$. Because B'_i is of dimension $R^{N\times 1}$, from Theorem 1 we know that projecting by each Q_i matches q moments of the output when input is J_is^i. So according to superposition theorem, projecting by Q_i can match q moments of output when input is J(s).

From the above proof we can see that the essence of MSMOR is to convert a MIMO circuit into SISO one with equivalent output. This is exactly the reason why MSMOR can outperform those MOR methods without considering RHS sources when there are multiple sources. When we reduce the circuit to order q, MSMOR can match the first q moments of the output vector, while those methods can only match $\lfloor \frac{q}{p} \rfloor$ moments.

As we have claimed previously, MSMOR is numerically more stable, more accurate and more efficient. First, in MSMOR the new vector is generated only by the othogonomalized previous one, thus avoiding the error amplification. Second, techniques as described in [9] can be employed to deal with the deflation cases. The iteration might continue even breakdown happens. Therefore, it can help to improve the stability of the orthonormalization process.

Here we present some further discussions about the time complexity of MSMOR comp ared with IEKS and EKS. We can easily find that MSMOR has a time complexity of $O(q)$, while IEKS and EKS has that of $O(q^2)$ due to the incremental orthogonalization process. So our method is more efficient when increasing the order.

4. NUMERICAL EXPERIMENT

In this section, we present several numerical experiments to demonstrate the efficiency and accuracy of the proposed method and compare it with EKS, IEKS and SAPOR [3], a second-order Arnoldi method without considering multiple sources. Both methods are implemented in MATLAB. Experiments are run on a PC with Intel Pentium IV 2.66G CPU and 1G RAM.

We first use a 4×4 RLC mesh grid with 192 nodes as the first example. We connect 50 ports with PWL sources, reduce the circuit to order 80, and measure the output of a randomly selected port. The PWL current sources are generated from real FPGA circuits. The frequency domain response is shown in Figure 1. From the figures we can conclude that MSMOR can match perfectly with the original curve, while IEKS shows a little difference at lower frequencies. EKS, although worse than IEKS, outperforms SAPOR significantly. This is because SAPOR can only match first block moment of the original system which illustrates the advantage of model order reduction with multiple sources.

We also perform time domain simulation and the results for a certain time period are provided in Figure 2. In this time period, the input PWL sources vanish and the output voltages approach to zero. It is clear that MSMOR's result matches that of the orginal well. The result of MSMOR approaches zero faster than the other methods, because we can see from Figure 1 that the output of MSMOR has the largest high frequency content compared with other methods.

To further demonstrate the power of MSMOR, we use the same RLC mesh above, only changing RHS sources to

# of nodes	# of sources	Cir Sim	EKS	IEKS	MSMOR
192	50	0.18s	0.11s	0.09s	0.08s
768	100	106s	10.4s	10.2s	7.6s
2048	200	362s	20.6s	20.4s	15.8s
11520	800	1164s	66.1s	65.2s	47.3s
69380	4000	N/A	384s	381s	295s

Table 1: Comparison of the reduction time under the same accuracy up to 50GHz.

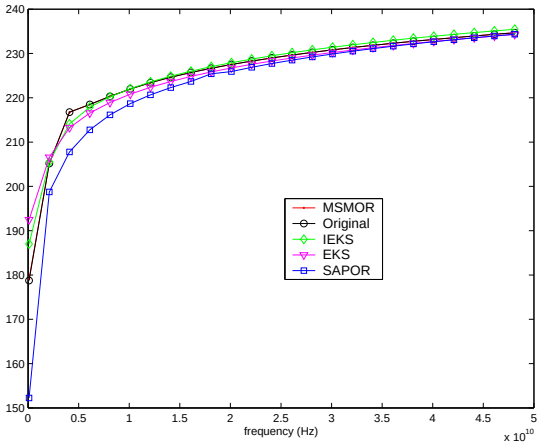

Figure 1: Frequency domain response comparison between MSMOR, IEKS, EKS, SAPOR and Original with PWL sources

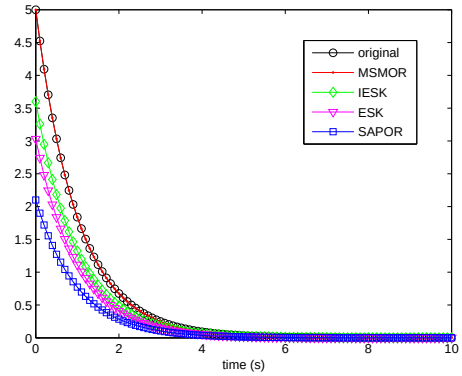

Figure 2: Time domain response comparison between MSMOR, IEKS, EKS, SAPOR and Original with PWL sources

attenuated sine waveforms. The result is shown in Figure 3. We exclude IESK here because it cannot handle sources with $\frac{1}{s^i}$ terms. From Figure 3 we can see MSMOR can still match the original output well. EKS, however, can only match well at DC and low frequency band. This is mainly because EKS can only take the first several moments of RHS sources to match and neglect the higher order terms which leads to a loss in high frequency band.

Figure 4 shows the average error of MSMOR, IEKS, EKS and SAPOR compared to the original result with respect to the reduced order. We perform test on several different size RLC meshes from 4×4 to 1024×1024 with PWL sources, and use the average as an indication. It is clear that MSMOR approaches to zero faster than IEKS and EKS. We also note that the error of SAPOR does not convergent with the increase of order. This is because it can only match the first block moment no matter how we raise the reduced order.

Another problem of major concern is the time complexity of MSMOR. Table 1 illustrates the run time comparison of MSMOR, EKS, IEKS, with respect to circuit size. It can be concluded that our MSMOR is more efficient than EKS and IEKS. The reason is stated in previous section.

We end the experiment section with a real package and power grid co-simulation example. An illustration of package and power grid is shown in Figure 5. It is one part from a real package design case. The size of the package is roughly 12000umx25000 and the granularity of the circuit is roughly 1500um.

5. CONCLUSION

In this paper, we presented MSMOR algorithm for the model order reduction of circuits with multiple sources. This method is more accurate compared to those algorithms that do not take multiple sources into consideration; And it outperforms the existing algorithms that deal with multiple sources, like EKS and IEKS, both in speed and in accuracy. What is more, to the best of our knowledge, this is the first algorithm that can deal with RCS circuits with multiple sources.

6. REFERENCES

[1] S. R. Nassif and J. N. Kozhaya, "Fast power grid simulation," in *Proc. Design Automation Conf. (DAC)*, 2000.

[2] A. Odabasioglu, M. Celik, and L. Pileggi, "PRIMA: Passive reduced-order interconnect macromodeling algorithm," *IEEE Trans. on Computer-Aided Design of Integrated Circuits and Systems*, pp. 645–654, 1998.

[3] B. Liu, X. Zeng, Y. Su, J. Tao, Z. Bai, C. Chiang, and D. Zhou, "Block sapor: Block second-order arnoldi method for passive order reduction of multi-input multi-output rcs interconnect circuits," in *Proc. Asia South Pacific Design Automation Conf. (ASPDAC)*, 2005.

[4] J. M. Wang and T. V. Nguyen, "Extended krylov subspace method for reduced order analysis of linear circuits with multiple sources," in *Proc. Design Automation Conf. (DAC)*, 2000.

[5] Y. Lee, Y. Cao, T. Chen, J. Wang, and C. Chen, "Hiprime: Hierarchical and passivity preserved interconnect macromodeling engine for rlkc power delivery," *IEEE Trans. on Computer-Aided Design of Integrated Circuits and Systems*, vol. 26, no. 6, pp. 797–806, 2005.

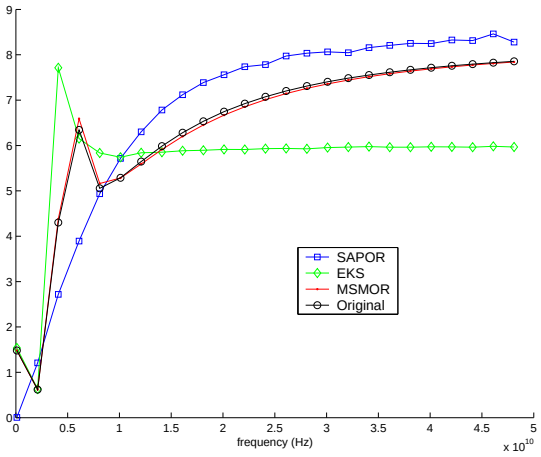

Figure 3: Frequency domain response comparison between MSMOR, EKS, SAPOR and Original with attenuated sine sources

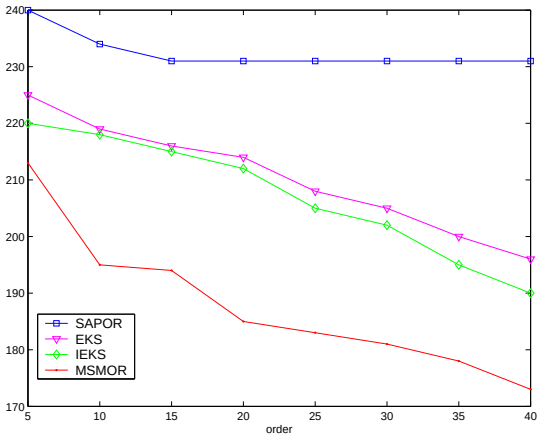

Figure 4: Error comparison between SAPOR, IEKS, EKS and MSMOR with respect to order

[6] D. Ling and A. Ruehli, *Circuit Analysis, Simulation and Design - Advances in CAD for VLSI*, vol. 3. Elsevier Science Publisher, 1987.

[7] A. Devgan, H. Ji, and W. Dai, "How to efficiently capture on-chip inductance effects: introducing a new circuit element K," in *Proc. Int. Conf. on Computer Aided Design (ICCAD)*, pp. 150–155, 2000.

[8] Y. Su, J. Wang, X. Zeng, Z. Bai, C. Chiang, and D. Zhou, "Sapor: Second-order arnoldi method for passive order reduction of rcs circuits," in *Proc. Int. Conf. on Computer Aided Design (ICCAD)*, 2004.

[9] Z. Bai and Y. Su, "Soar: A second-order arnoldi method for the solution of the quadratic eigenvalue problem," *SIAM J. Matrix Anal. Appl.*, vol. 26, no. 3, pp. 640–659, 2005.

[10] B. N. Sheehan, "Enor: Model order reduction of rlc circuits using nodal equations for efficient factorization," in *Proc. Design Automation Conf. (DAC)*, 1999.

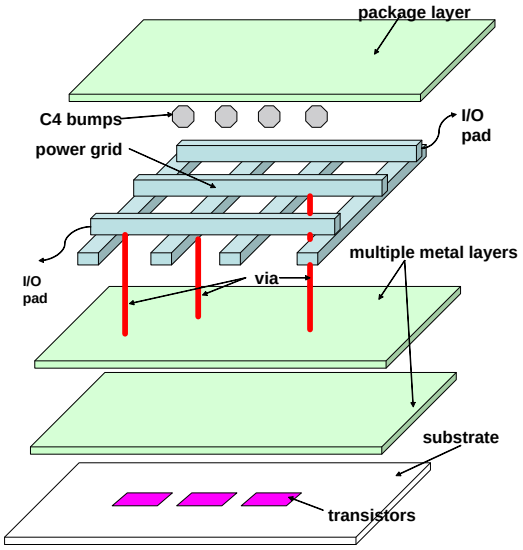

Figure 5: A simple illustration of package and power grid